Preprint

Temporally specific gene expression and chromatin remodeling programs regulate a conserved *Pdyn* enhancer

Robert A. Phillips III[1], Ethan Wan[1], Jennifer J. Tuscher[1], David Reid[1], Lara Ianov[1,2], Jeremy J. Day[1]*

Summary: Neuronal and behavioral adaptations to novel stimuli are regulated by temporally dynamic waves of transcriptional activity, which shape neuronal function and guide enduring plasticity. Neuronal activation promotes expression of an immediate early gene (IEG) program comprised primarily of activity-dependent transcription factors, which are thought to regulate a second set of late response genes (LRGs). However, while the mechanisms governing IEG activation have been well studied, the molecular interplay between IEGs and LRGs remain poorly characterized. Here, we used transcriptomic and chromatin accessibility profiling to define activity-driven responses in rat striatal neurons. As expected, neuronal depolarization generated robust changes in gene expression, with early changes (1 h) enriched for inducible transcription factors and later changes (4 h) enriched for neuropeptides, synaptic proteins, and ion channels. Remarkably, while depolarization did not induce chromatin remodeling after 1 h, we found broad increases in chromatin accessibility at thousands of sites in the genome at 4 h after neuronal stimulation. These putative regulatory elements were found almost exclusively at non-coding regions of the genome, and harbored consensus motifs for numerous activity-dependent transcription factors such as AP-1. Furthermore, blocking protein synthesis prevented activity-dependent chromatin remodeling, suggesting that IEG proteins are required for this process. Targeted analysis of LRG loci identified a putative enhancer upstream of *Pdyn*, a gene encoding an opioid neuropeptide implicated in motivated behavior and neuropsychiatric disease states. CRISPR-based functional assays demonstrated that this enhancer is both necessary and sufficient for *Pdyn* transcription. This regulatory element is also conserved at the human *PDYN* locus, where its activation is sufficient to drive *PDYN* transcription in human cells. These results suggest that IEGs participate in chromatin remodeling at enhancers and identify a conserved enhancer that may act as a therapeutic target for brain disorders involving dysregulation of *Pdyn*.

INTRODUCTION

Experience-dependent cellular adaptations within the brain circuits that control motivated behaviors are critical for learning, memory, and long-term behavioral change. In psychiatric disorders such as drug addiction, these cellular changes are hijacked to drive maladaptive behavioral changes that promote drug seeking[1,2]. Furthermore, mutations that alter the function of activity-dependent transcription factors have been implicated in a host of neurodevelopmental and autism spectrum disorders[3,4]. Adaptations to novel stimuli are regulated by temporally and functionally distinct activity-dependent transcriptional programs. For example, various forms of neuronal activation result in the rapid induction of immediate early genes (IEGs), including transcription factors such as *Fos* (aka c-Fos), *Npas4*, and *Nr4a2*. These genes follow a temporally dynamic profile, with elevated expression within 1 h of a stimulus and rapid return to baseline levels. In contrast, the same stimuli promote expression of a more delayed gene expression program, termed late response genes (LRGs)[5,6]. This set of genes includes kinases, neurotrophic factors, and neurotransmitter receptors. Current models of activity-dependent gene expression suggest that these distinct transcriptional waves work together to promote enduring cellular and behavioral adaptations.

While genes within the IEG expression program are required for cellular and behavioral changes following stimulation, the exact mechanisms by which they contribute to LRG expression and the functional consequences of this process remain poorly characterized. Recent evidence suggests that chromatin remodeling at genomic enhancers is a key event linking LRGs to IEGs[7,8]. In non-neuronal systems, AP-1, an activity-dependent transcription factor consisting of *Fos* and *Jun* family members, directly contributes to chromatin remodeling at LRG enhancers[7]. However, despite ample evidence for activity-dependent transcription of AP-1 members in multiple brain regions and cell types, understanding the nature and functional consequences of LRG induction remains a challenge for several reasons. First, emerging evidence has revealed that different classes of neurons induce distinct LRG programs in response to the same neuronal activation. Second, different types of stimuli

[1]*Department of Neurobiology, University of Alabama at Birmingham, Birmingham, AL 35294, USA*
[2]*Civitan International Research Center, University of Alabama at Birmingham, Birmingham, AL 35294, USA*
**Correspondence to Jeremy Day* (jjday@uab.edu | day-lab.org | @DayLabUAB)

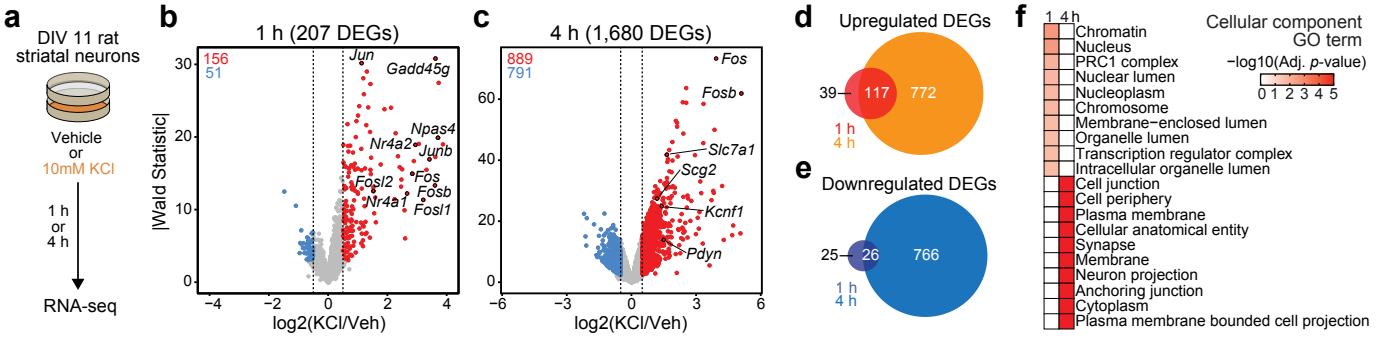

Figure 1. Characterization of temporally and functionally distinct activity-dependent gene expression programs in cultured striatal neurons. **a**, Experimental design. DIV11 cultures were depolarizated for 1 or 4 h with 10mM KCl. Following treatment, RNA-seq libraries were constructed. **b-c**, Volcano plots displaying gene expression changes after 1 and 4 h of neuronal depolarization. **d-e**, Venn diagrams comparing 1 and 4 h upregulated and downregulated DEGs. **f**, Top 10 cellular component GO terms for 1 and 4 h upregulated DEGs.

may give rise to non-overlapping constellations of IEG transcription factors, which could promote activation of distinct LRGs to tune neuronal responses. Finally, even where chromatin remodeling has been identified near LRGs, the consequences of this remodeling have not been concretely linked to transcriptional activation of candidate LRGs.

Here, we used next generation sequencing approaches to characterize temporally distinct, activity-dependent transcriptomic and epigenomic reorganization in cultured rat embryonic striatal neurons, an *in vitro* model containing many cell types implicated in learning, motivation, reward, and substance use disorders[9]. These experiments comprehensively characterized activity-responsive genes in both the IEG and LRG expression programs in striatal neurons, and revealed a temporal decoupling between IEG activation and activity-dependent chromatin remodeling. Further functional studies suggest that translation of IEGs is necessary for activity-dependent chromatin remodeling, and that sites of chromatin opening are enriched for AP-1 transcription factor motifs. Combining transcriptional and epigenomic profiling allowed us to identify a putative enhancer upstream of the *Pdyn* locus that is conserved in the human genome. CRISPR-based activation and repression experiments provided functional validation that this region serves as a *Pdyn* enhancer in both rat neurons and dividing human cell lines. Collectively, these results highlight the mechanisms through which neuronal activity promotes gene expression changes to modify neuronal function, and have relevance for brain disease states characterized by alterations to this process.

RESULTS

Characterization of temporally and functionally distinct transcriptional programs following neuronal depolarization

Activity-dependent transcriptomic and epigenomic reorganization has been heavily implicated in neuropsychiatric diseases, such as drug addiction. Previously, our lab established cultured rat embryonic striatal neurons as an *in vitro* model for studying activity-dependent processes as these cultures contain the same cell types affected by drugs of abuse in the rat ventral striatum[9]. To characterize IEG and LRG expression programs in this model system, we performed RNA-seq following neuronal depolarization with 10mM KCl for 1 or 4 h (**Fig. 1a**). Following 1 h of depolarization, we identified 207 differentially expressed genes (DEGs; defined as genes with an adjusted p-value < 0.05 and |log2FoldChange| > 0.5). Notably, ~75% of these genes were upregulated by KCl, including activity-dependent transcription factors such as *Npas4*, *Fos*, *Fosb*, *Fosl2*, and *Nr4a1* (**Fig. 1b, Table S1**). In contrast, 4 h of depolarization resulted in significant transcriptomic reorganization, with 1,680 genes identified as DEGs (**Fig. 1c, Table S1**). DEGs upregulated by KCl at this timepoint included the opioid propeptide *Pdyn*, as well as the voltage-gated potassium channel *Kcnf1* (**Fig. 1c**). Interestingly, overlap between 1 h DEGs (putative IEGs) and 4 h DEGs (putative LRGs) primarily occurred when IEGs such as *Fos* were upregulated at both 1 and 4 h (**Fig. 1d,e; Fig. S1a**). In contrast, most 4 h DEGs such as *Pdyn* demonstrated temporally specific upregulation and were only activated following 4 h of depolarization (**Fig. S1b**).

To determine whether 1 h and 4 h specific DEGs were functionally distinct, we used gProfiler[10] to identify enriched cellular component and molecular function gene ontology (GO) terms in each gene list. 1 h DEGs, or IEGs, were enriched for cellular component terms such as "Nucleus", "Chromatin", and "Transcription regulator complex" (**Fig. 1f**), suggesting that most DEGs were transcription factors or genes encoding proteins involved in transcriptional regulation. Conversely, 4 h DEGs, or LRGs, were enriched for cellular component terms such as "Synapse" and "Neuron projection" (**Fig. 1f**), suggesting that these DEGs encode proteins required for cellular adaptations to stimulation. Molecular function GO term analysis found overlap between IEGs and LRGs (**Fig. S1c**), with both IEG-specific and overlapping molecular function GO terms including transcription factor activity (**Table S2**). However, LRG molecular function GO terms were distinct and included "voltage gated channel activity" and "G protein-coupled receptor binding" (**Table S2**). Together, these results demonstrate that striatal neuron depolarization induces temporally and functionally

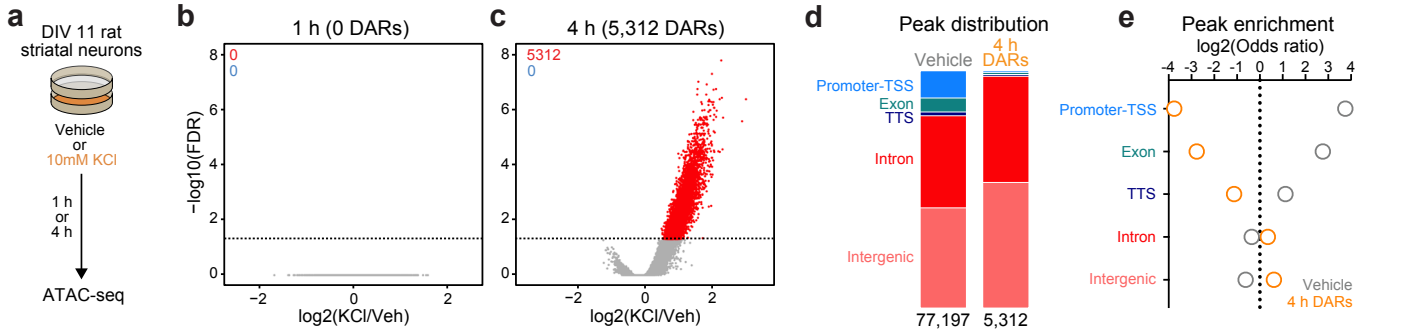

Figure 2. Activity-dependent chromatin remodeling in cultured primary rat striatal neurons. **a**, DIV11 primary rat striatal neurons were treated with 10mM KCl for 1 or 4 h. Following treatment, ATAC-seq libraries were prepared. **b-c**, Volcano plots displaying differentially accessible regions (DARs) after 1 and 4 h of neuronal depolarization. **d**, Genomic location of vehicle and 4 h DAR ATAC peaks. **e**, Odds ratio for genomic annotations of 4 h DARs or vehicle peaks.

distinct gene expression programs that can be classified as IEGs and LRGs.

Activity-dependent chromatin remodeling primarily occurs in non-coding genomic regions

In non-neuronal systems, LRG induction is dependent on activity-dependent chromatin remodeling at genomic enhancers[7]. To identify the potential mechanisms governing transcriptomic reorganization following 4 h of depolarization, we first sought to identify whether activity-dependent chromatin remodeling occurs in striatal neurons. Cultured rat embryonic striatal neurons were treated with 10mM KCl for 1 or 4 h and assay for transposase accessible chromatin followed by next generation sequencing (ATAC-seq) libraries were prepared (**Fig. 2a**). Strikingly, 1 h of depolarization did not induce any chromatin remodeling that passed genome-wide cutoffs for statistical significance (**Fig. 2b**). However, 4 h of depolarization induced genome-wide chromatin remodeling with 5,312 differentially accessible regions (DARs, defined as regions with adjusted p-value ≤ 0.05), all of which become more open with depolarization (**Fig. 2c**; **Table S3**). Previous studies have suggested that activity-dependent chromatin remodeling and other epigenetic processes occur in non-coding regions associated with genomic enhancers[7,11,12]. To understand whether activity-dependent chromatin remodeling preferentially occurred in non-coding genomic regions, we calculated the odds ratio of enrichment compared to chance levels for all 4 h DARs as well as baseline peaks identified in vehicle treated samples that did not overlap 4 h DARs (termed "vehicle" peaks; **Fig. 2d**). Notably, vehicle peaks were significantly enriched in coding regions and proximal promoters (**Fig. 2e**). In contrast, activity-regulated DARs were depleted in coding regions and promoters, but were enriched in intergenic and intronic regions of the genome. This distribution is consistent with a function for these DARs as distal cis-regulatory enhancer elements.

Enhancers are marked by distinctive histone modifications, including histone acetylation (at H3K27) and increased ratios of histone monomethylation to trimethylation at H3K4 (H3K4me1:H3K4me3). In contrast, while promoters are also marked by H3K27ac, they tend to exhibit a lower H3K4me1:H3K4me3 ratio[13,14]. To investigate whether 4 h DARs were enriched for enhancer-associated histone modifications, we next leveraged a recent study[15] that profiled histone modification enrichment throughout the mouse striatum. While DARs and vehicle peaks were enriched for H3K27ac and H3K4me1 (**Fig. S2a,b**), DARs had a significantly higher H3K4me1:H3K4me3 ratio than vehicle peaks (**Fig. S2c,d**). The preferential enrichment of DARs in non-coding regions coupled with the presence of H3K27ac and increased ratios of H3K4me1:H3K4me3 suggests that activity-dependent chromatin remodeling occurs at genomic enhancers in striatal neurons.

Transcription factor motifs associated with IEGs are significantly enriched in 4 h DARs

The combination of RNA-seq and ATAC-seq results suggests a temporal decoupling between induction of IEG transcription factors and activity-dependent chromatin remodeling. IEG transcription factors were activated following 1 h of depolarization (**Fig. 1b**), but activity-dependent chromatin remodeling only occurred following 4 h of depolarization (**Fig. 2c**). Furthermore, IEG transcription factors are critical mediators of activity-dependent chromatin remodeling in neuronal[8] and non-neuronal cells[7]. Thus, we predicted that IEG transcription factor motifs would be enriched in 4 h DARs.

To test this possibility, we searched for enriched motifs using a database of experimentally validated transcription factor binding motifs with HOMER[16]. Additionally, because millions of IEG motifs are found throughout the genome, we compared the enrichment between 4 h DARs and peaks found in vehicle treated samples. HOMER uses randomly selected background regions to compare the enrichment of motifs within a user identified peak set. This allowed us to calculate a percent enrichment, or the percent of background sequences with the motif subtracted from percent of target sequences with the motif. While no transcription factor motifs exhibited enrichment greater than 50% in the vehicle peak dataset (**Fig. 3a**), 8 motifs exceed this threshold within 4 h DARs (**Fig. 3b**). Interestingly, all motifs correspond to versions of the consensus motif for the AP-1 family of activity-dependent transcription factors, with 93% of 4 h DARs containing an AP-1

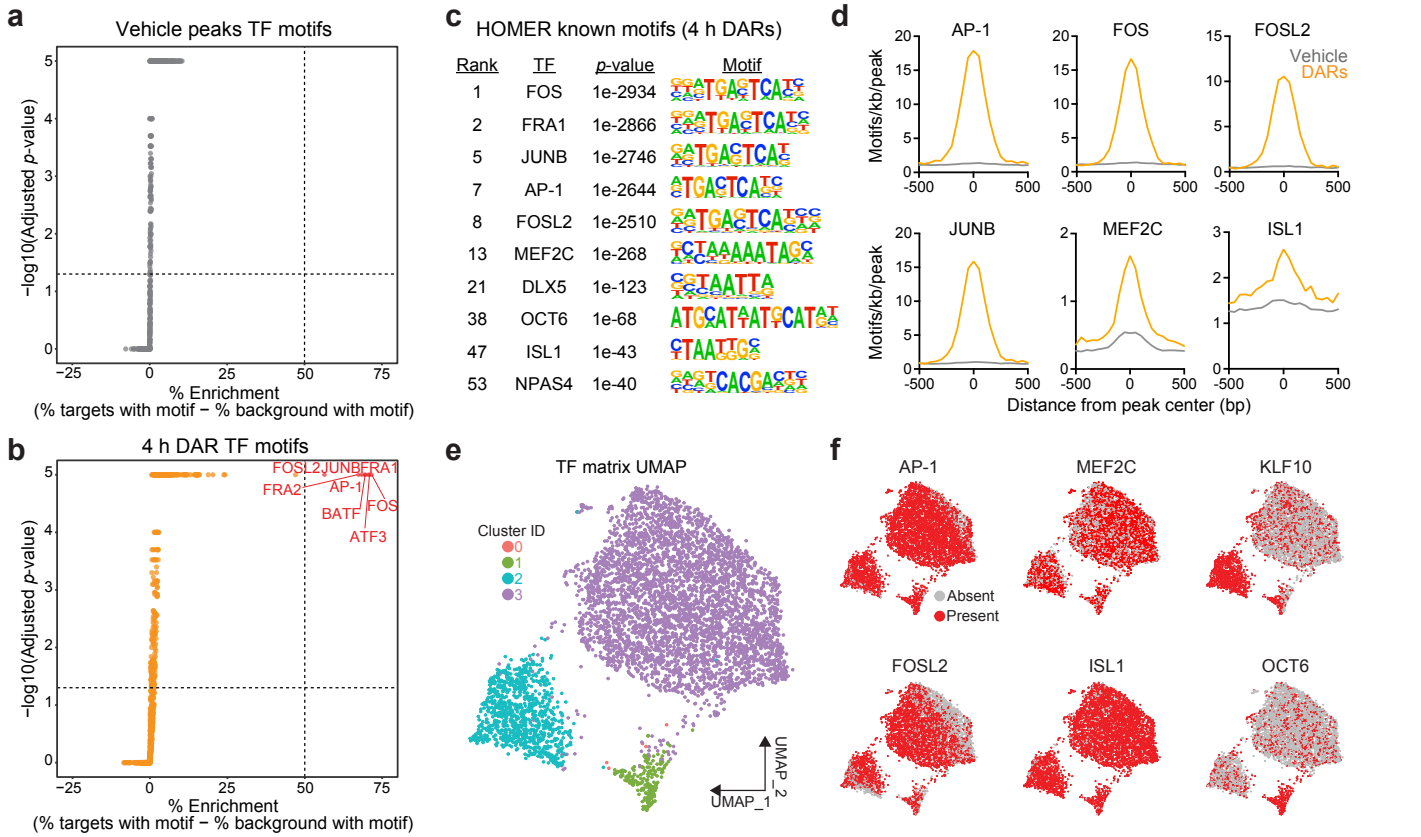

Figure 3. Motifs for activity-dependent transcription factors are significantly enriched in 4 h DARs. **a-b**, Plots showing enrichment of specific transcription factor motifs in vehicle peaks and 4 h DARs. Motifs with significant adjusted p-values and a percent enrichment greater than 50% are shown in red and labeled with the corresponding transcription factor. **c**, Representative results from HOMER known motif enrichment analysis conducted using 4 h DAR peak set. **d**, Motifs for activity-dependent TFs (AP1, FOS, FOSL2, JUNB), MEF2C, and ISL1 are enriched at the center of DARs. **e**, UMAP generated using transcription factor motif enrichment within the 4 h DARs. **f**, UMAPs colored by the presence of absence of specific transcription factor motifs. KLF10 and OCT6 specifically mark clusters 2 and 1, respectively.

motif (**Fig. 3c**). In addition to calculation of a percent enrichment, we calculated the enrichment of specific motifs across DARs and vehicle peaks. AP-1, as well as its subunits FOS, FOSL2, and JUNB, were significantly enriched at the center of DARs and not in vehicle peaks (**Fig. 3d**). Recently, binding sites for the AP-1 family member ΔFosB were assayed in the adult mouse nucleus accumbens using CUT&RUN[15]. Bindings sites identified in this study were then mapped to the rat genome. ΔFosB is significantly enriched in DARs, but not in vehicle peaks or a set of 5,312 random regions that are the same size as DARs (**Fig. S2e**). Additional analyses identified that MEF2C motifs were enriched at the center of DARs (**Fig. 3c-d**). MEF2C is a member of the MEF2 family of proteins that are integral regulators of synaptic plasticity in the developing brain and interact with histone deacetylases to alter chromatin accessibility[4,17,18]. ISL1, is an integral regulator of MSN development[19], was also enriched at the center of DARs, with 95% of DARs containing an ISL1 motif (**Fig. 3c-d**).

The HOMER database allowed us to investigate the enrichment of over 400 transcription factor motifs in over 5,300 DARs. To understand if DARs could be separated based on the transcription factor motifs present within these regions, we used uniform manifold approximation and projection (UMAP; a dimensionality reduction technique)[20] and density-based clustering[21] to separate DARs based on the presence, absence, or count of annotated transcription factor motifs. This analysis identified 3 major clusters with some DARs labeled as outliers (cluster 0) (**Fig. 3e**). Unsurprisingly, clusters were not defined by the presence of AP-1, FOSL2, MEF2C, or ISL1, transcription factors that are significantly enriched at the center of DARs (**Fig. 3f**). However, cluster 2 was marked by the presence of the KLF10 motif and cluster 1 was marked by the presence of a motif corresponding to OCT6 (**Fig. 3f**). Taken together, these results demonstrate a significant enrichment of IEG motifs within 4 h DARs and suggests that IEGs may participate in activity-dependent chromatin remodeling in striatal neurons.

De novo protein translation is required for activity-dependent chromatin remodeling

The significant enrichment of IEG transcription factor motifs within 4 h DARs suggests that these inducible transcription factors may be required for subsequent activity-dependent chromatin remodeling. Furthermore, the temporal decoupling between IEG expression and activity-dependent chromatin remodeling suggests that IEGs must be translated before acting on genomic regions to induce an open chromatin state. To test the hypothesis that *de novo* protein translation is required for activity-dependent chromatin remodeling, we repeated ATAC-seq after 4 h of depolarization in combination with protein synthesis

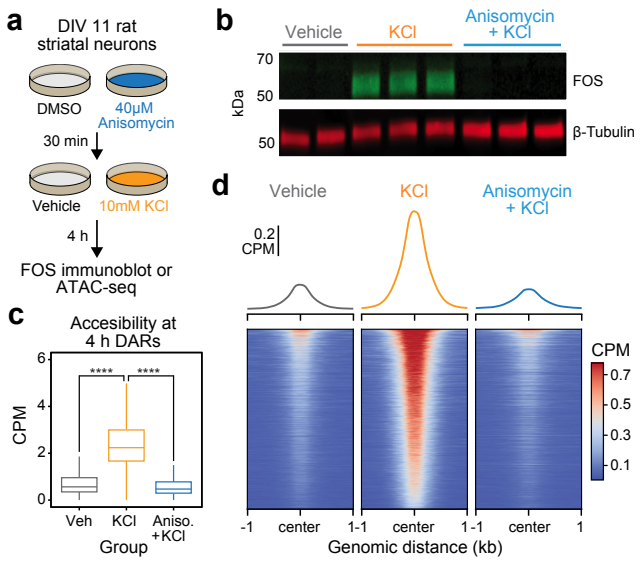

Figure 4. Activity-dependent chromatin remodeling requires protein translation. **a**, Experimental design. DIV11 primary rat striatal neurons were treated with DMSO or anisomycin for 30 minutes followed by 4 h of depolarization with 10mM KCl. **b**, Western blot for FOS and β-tubulin from striatal neurons treated with vehicle, 10mM KCl, or 10mM KCl + 40 μM Anisomycin. **c**, Boxplots demonstrating the effects of anisomycin on activity-dependent chromatin remodeling. One way ANOVA with Tukey's multiple comparisons test, ****p<0.0001. **d**, Heatmaps and mean accessibility plots from 4 h DARs. For heatmaps, each row represents a single DAR. CPM = counts per million.

inhibition. Cultured rat embryonic striatal neurons were pretreated with 40μM anisomycin, a translation inhibitor, for 30 minutes followed by 10mM KCl for 4 h (**Fig. 4a**). As expected, 40μM anisomycin was sufficient to block depolarization-induced translation of FOS protein, as determined by immunoblotting (**Fig. 4b**). Targeted analysis of the previously identified 5,312 DARs demonstrated replication of activity-dependent chromatin remodeling at these regions (**Fig. 4c**). Pretreatment with anisomycin completely blocked activity-dependent chromatin remodeling across the genome (**Fig. 4c,d**), demonstrating that *de novo* protein translation is required for activity-dependent changes in chromatin accessibility. Further, this result suggests that chromatin remodeling induced by neuronal depolarization is regulated by IEG transcription factors.

Activity-dependent Pdyn transcription is regulated by IEGs and protein translation

Given that activity-dependent chromatin remodeling across the genome required protein translation, we next sought to identify discrete regions near LRGs that may serve as activity-dependent enhancers. We predicted that regions serving as activity-dependent enhancers for LRGs would be: 1) located in non-coding regions of the genome, 2) inaccessible at baseline and accessible following depolarization, and 3) inaccessible when depolarization was paired with protein synthesis inhibition. These regions would be fundamentally different from enhancers regulating IEGs (such as the enhancers within the *Fos* locus), which are accessible at baseline and do not undergo activity-dependent chromatin remodeling (**Fig. S3**). We identified a putative enhancer ~45 kilobases upstream of the *Pdyn* TSS that met all of these criteria (**Fig. 5a**). While *Pdyn* is an LRG that plays important roles in striatal function, the *Pdyn* promoter does not undergo activity-dependent chromatin remodeling (**Fig. 5a**). Next, we predicted that if this differently accessible chromatin region in the *Pdyn* locus serves as enhancer for *Pdyn*, then blocking protein translation should also attenuate activity-dependent *Pdyn* transcription. In support of this prediction, anisomycin pretreatment completely blocked activity-dependent *Pdyn* transcription, as detected with RT-qPCR (**Fig. 5b**). Additionally, anisomycin pretreatment attenuated baseline *Pdyn* mRNA levels in the absence of stimulation, suggesting that basal *Pdyn* expression is comprised of both constitutive and activity-dependent transcriptional events (**Fig. 5b**).

To determine whether *Pdyn* is directly regulated by IEG transcription factors, we leveraged a previously published RNA-seq dataset that used CRISPR activation tools to overexpress 16 IEGs that are upregulated in striatal neurons following dopamine stimulation[9] (**Fig. 5c**). CRISPR-based activation of 16 IEGs (including *Fos*, *Fosb*, and *Junb*) resulted in significant upregulation of *Pdyn* mRNA (**Fig. 5d**), demonstrating that activation of IEGs is sufficient to upregulate *Pdyn* expression. To further investigate the transcriptional regulation of *Pdyn*, we leveraged a publicly available single nucleus RNA-sequencing dataset from rats treated with a single dose of cocaine (or saline as a control; **Fig. 5e**)[9]. Because these rats were sacrificed one hour after injection, we reasoned that LRGs have not yet been fully activated by cocaine experience at this timepoint. However, using pseudotime analysis to reconstruct gene regulatory networks allowed us to identify predicted upstream regulators of *Pdyn* transcription. In prior work, we demonstrated that distinct populations of Drd1-MSNs have differential responses to cocaine[22]. Therefore, pseudotime trajectory graphs were constructed such that the highest pseudotime marked cells that were transcriptionally activated by cocaine (i.e., expressed high levels of IEGs) (**Fig. 5f-g**). *Pdyn* mRNA levels were also higher in cells with high *Fos* and *FosB* expression (**Fig. 5g**). Finally, a gene regulatory network was constructed for cells with high IEG levels. This network predicted that the IEG transcription factors *Fos*, *Fosb*, *Fosl2*, *Nr4a1*, and *Nr4a2* all regulate *Pdyn* (**Fig. 5h**). As a positive control, we also generated a gene regulatory network for *Scg2*, an LRG that was previously demonstrated to be regulated by *Fos*[23]. This network also predicted *Fos* as a regulator of *Scg2* (**Fig. S4**), demonstrating that this computational technique can replicate experimental findings.

CRISPR-based functional validation of a novel Pdyn enhancer

The observation that *Pdyn* DAR accessibility and *Pdyn* mRNA were both activity- and translation-dependent suggests that this site acts as a stimulus-regulated enhancer for *Pdyn*. To test this hypothesis, we used a catalytically dead version of Cas9 (dCas9) fused to the transcriptional activator VPR (CRISPRa) or the

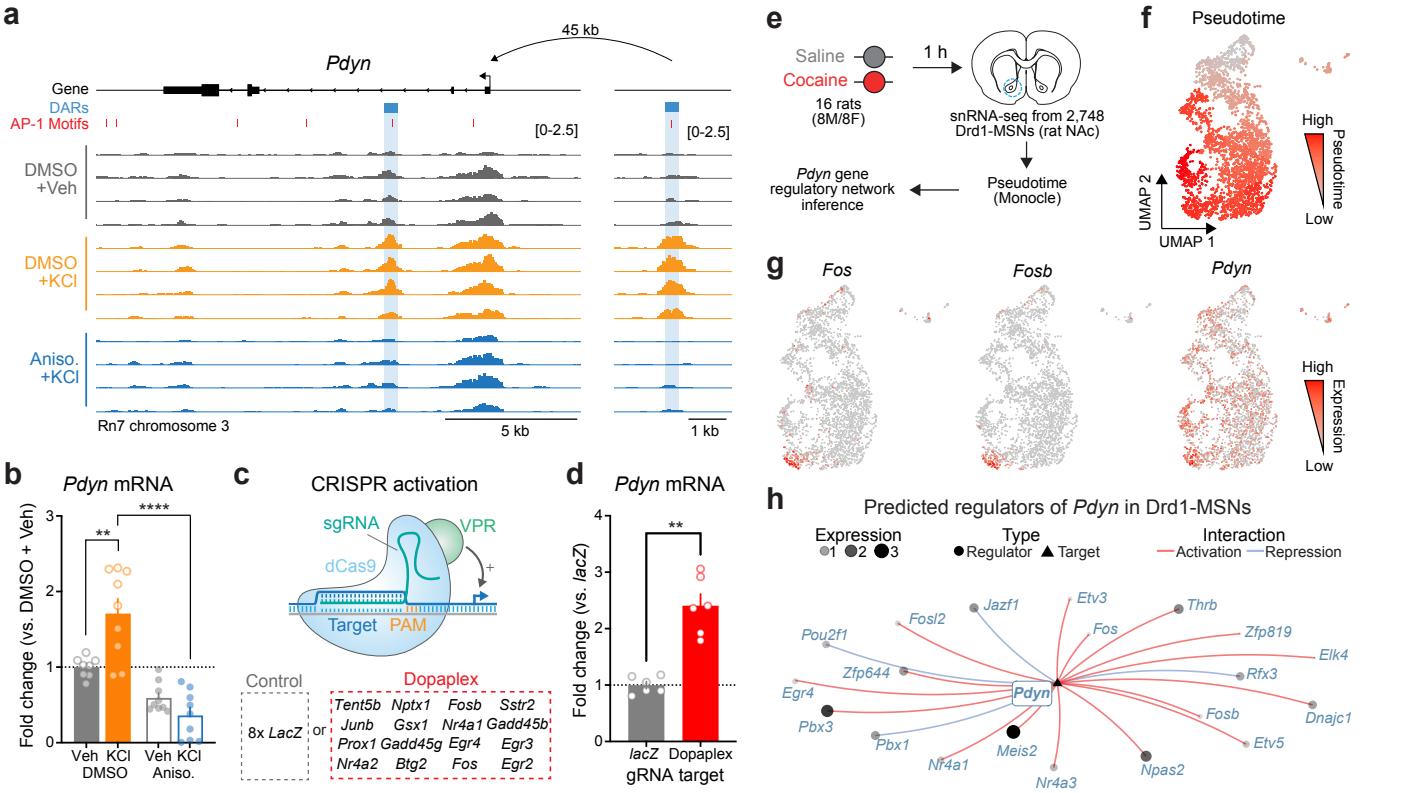

Figure 5. Transcriptional regulation of *Pdyn* mRNA. **a**, ATAC-seq tracks at the *Pdyn* gene locus of embryonic striatal neurons treated with DMSO + Vehicle, DMSO + KCl, or anisomycin + KCl. A DAR 45 kb upstream of the *Pdyn* TSS in a non-coding region becomes accessible with depolarization only with intact protein translation. **b**, RT-qPCR for *Pdyn* mRNA from DIV 11 rat striatal neurons treated with vehicle, KCl, anisomycin, or anisomycin + KCl. Induction of *Pdyn* mRNA by KCl is blocked by anisomycin pretreatment (One-way ANOVA with Tukey's multiple comparisons test **p<0.01, ****p<0.0001). **c**, Targeted activation of dopamine-regulated immediate early genes with CRISPR activation (data from reference *9*). dCas9-VPR was transduced with multiplexed sgRNAs targeting 16 immediate early genes. **d**, *Pdyn* mRNA is upregulated following CRISPR-based activation of 16 IEGs. Mann-Whitney Test **p<0.01. **e**, Pseudotime analysis to predict regulators of *Pdyn* expression in Drd1-MSNs was performed with avaialable snRNA-seq data from the rat nucleus accumbens[9]. **f-g**, Feature plots for Pseudotime, *Fos*, *Fosb*, and *Pdyn* in Drd1-MSNs. **h**, Gene regulatory network reconstruction from single cell trajectories identifies predicted regulators of *Pdyn* in Drd1-MSNs.

transcriptional repressor KRAB-MeCP2 (CRISPRi)[24,25] to activate or silence this region on demand (**Fig. 6a,b**). To test the necessity of the DAR in mediating activity dependent *Pdyn* transcription, we used single guide RNAs (sgRNAs) to target dCas9-KRAB-MeCP2 to the DAR in the presence of depolarization. As a negative control, we transduced cultured striatal neurons with a sgRNA for *lacZ*, a bacterial gene not found in the mammalian genome. As expected, activity-dependent *Pdyn* upregulation was observed in neurons transduced with *lacZ* sgRNAs and dCas9-KRAB-MeCP2 (**Fig. 6c**). However, KCl-induced *Pdyn* upregulation was blocked in neurons transduced with DAR-targeting sgRNAs and dCas9-KRAB-MeCP2 (**Fig. 6c**). Additionally, baseline *Pdyn* mRNA levels were attenuated by CRISPRi of the *Pdyn* DAR (**Fig. 6c**), suggesting that this enhancer may be accessible at baseline in some cells or as a consequence of spontaneous neuronal activity. These results demonstrate that the DAR upstream of the *Pdyn* TSS is necessary for activity-dependent *Pdyn* transcription.

Next, we transduced neurons with the same sgRNAs targeting *lacZ* or the *Pdyn* DAR and dCas9-VPR (CRISPRa) to test if activation of this DAR is sufficient to promote *Pdyn* transcription. *Pdyn* mRNA levels were significantly increased in neurons transduced with DAR-targeting sgRNAs (**Fig. 6d**), demonstrating that transcriptional activation of the DAR is sufficient for upregulation of *Pdyn* mRNA levels. To test the specificity of the DAR for regulation of *Pdyn*, we also measured mRNA levels of the two closest genes within the *Pdyn* locus, *Sirpa* and *Stk35*. CRISPRa based transcriptional activation of the DAR did not result in significant upregulation of *Sirpa* or *Stk35*. Taken together, these CRISPR-based functional assays demonstrate that the DAR upstream of the *Pdyn* TSS is a genomic enhancer that is necessary, sufficient, and specific for *Pdyn* transcription.

PDYN is a cell type-specific LRG in the human genome regulated by a conserved genomic enhancer

Because genomic enhancers are critical regulators of genes important for shared biological functions, many of these elements are conserved across species. Furthermore, regions undergoing activity-dependent chromatin remodeling in human neurons harbor genetic variants associated with the development of neuropsychiatric disorders[26]. Thus, we next set out to understand if *PDYN* is an LRG in the human genome, and whether the identified rat enhancer is conserved. To test whether *PDYN* is an LRG in the human genome, we leveraged publicly available RNA-seq datasets from cultured human GABAergic neurons[26]. These neurons were depolarized for 0.75 or 4 h, timepoints that allow for the investigation of IEGs and LRGs, respectively. Like cultured rat embryonic striatal neurons, *PDYN* is

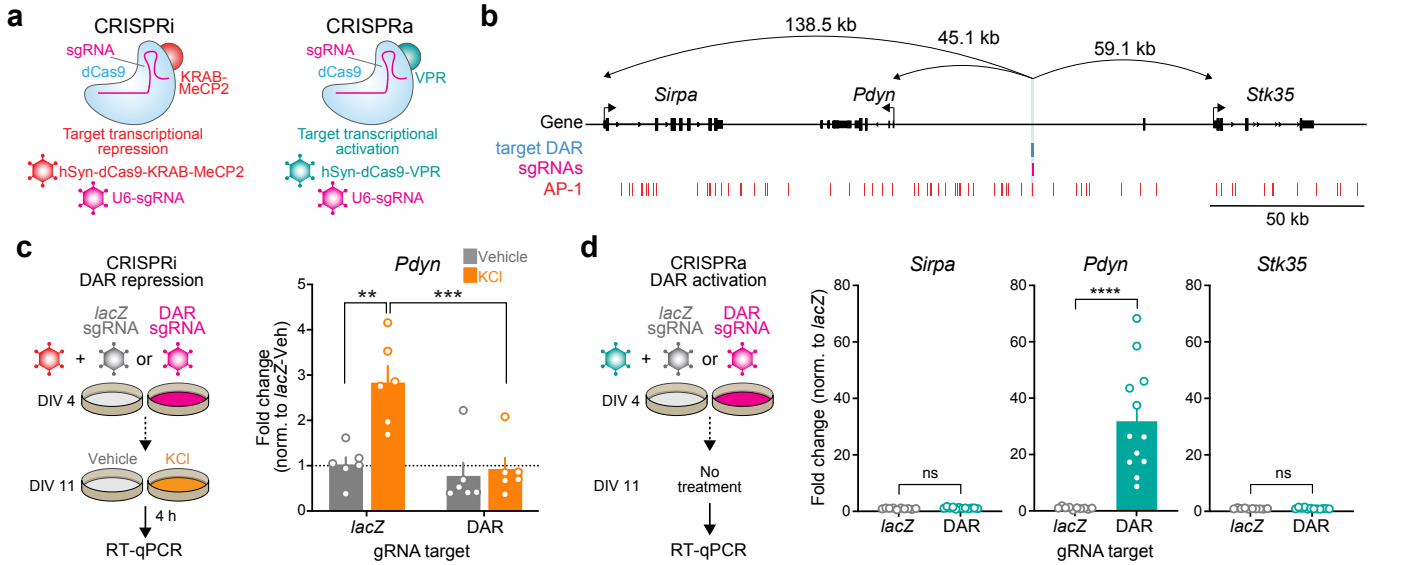

Figure 6. CRISPR-based functional validation of a novel *Pdyn* enhancer. **a**, Viral strategy for functional validation of putative enhancers using CRISPR interference with dCas9-KRAB-MeCP2 and CRISPR activation with dCas9-VPR. **b**, CRISPR sgRNAs (4x) were designed to target the activity-regulated DAR 45.1 kb upstream of *Pdyn* in the rat genome. **c**, CRISPRi at the *Pdyn* DAR blocks activity-dependent induction of *Pdyn* mRNA. Cultured embryonic striatal neurons were transduced with dCas9-KRAB-MeCP2 and sgRNAs targeting *lacZ* (non-targeting control) or the *Pdyn* DAR. Neurons were then treated with vehicle or 10mM KCl for 4 h prior to RT-qPCR. One-way ANOVA with Tukey's multiple comparisons test $^{**}p<0.01$, $^{***}p<0.001$. **d**, CRISPRa at the *Pdyn* DAR selectively upregulates *Pdyn* mRNA without altering expression of the nearest upstream and downstream genes. Striatal neurons were transduced with dCas9-VPR and sgRNAs targeting *lacZ* or the *Pdyn* DAR. Folowing RNA extraction at DIV 11, RT-qPCR was used to measure expression of *Pdyn*, *Sirpa*, and *Stk35*. Mann-Whitney test ****p<0.0001.

only upregulated following 4 h of depolarization (**Fig. 7a-c**). This study also performed the same experiments in cultured human glutamatergic neurons, allowing us to investigate whether PDYN is a cell type-specific LRG. Analysis of *PDYN* at several timepoints in both glutamatergic and GABAergic neurons demonstrated that *PDYN* is only upregulated in GABAergic neurons following 4 h of depolarization (**Fig. 7d**).

This published study also performed ATAC-seq on human glutamatergic and GABAergic neurons following 0 and 90 minutes of depolarization. While 90 minutes does not provide the same temporal resolution for chromatin remodeling at genomic enhancers as our experiments in rat neurons, it is a timepoint in which chromatin remodeling may initially occur following stimulation. Interestingly, the rat *Pdyn* DAR is conserved in a region that is also upstream of the human *PDYN* TSS (**Fig. 7e**), and this region undergoes time-dependent increases in chromatin accessibility following KCl stimulation along with other identified DARs in this locus (**Fig. 7f**). Furthermore, activity-induced chromatin remodeling at the conserved and experimentally validated DAR only occurs in human GABAergic neurons (**Fig. S5**). To test if this enhancer is sufficient for upregulation of *PDYN* transcription in human cells, we transfected HEK-293T cells with plasmids to express dCas9-VPR machinery and sgRNAs targeting the conserved region (**Fig. 7g**). Transcriptional activation of the conserved DAR was sufficient to upregulate human *PDYN* transcription (**Fig. 7h**). Together, these results suggest that *PDYN* is a cell type-specific LRG within the human genome that is regulated by a conserved enhancer element.

Pdyn enhancer is accessible in the adult rat striatum in a cell type-specific manner

To determine whether the activity-dependent *Pdyn* enhancer characterized *in vitro* is also functional in the adult brain, we performed snATAC-seq using nuclei from male and female adult Sprague-Dawley rats that received once daily intraperitoneal cocaine injections for 7 consecutive days (repeated cocaine; **Fig. 8a**). 10,085 snATAC-seq nuclei were sequenced and integrated with a previously published snRNA-seq dataset that contained NAc nuclei from rats treated with repeated cocaine injections[27] to identify cell types. Nuclei were distributed across 14 distinct cell types (**Fig. 8b**) that include previously identified neuronal and non-neuronal cell populations[9,27]. Visualization and accessibility peak-calling identified that the validated *Pdyn* enhancer locus was accessible in both Drd1- and Grm8-MSNs (**Fig. 8b**), populations that also express high levels of *Pdyn* at the mRNA level. Furthermore, co-accessibility analysis identified that accessibility of the *Pdyn* enhancer was correlated with accessibility of the *Pdyn* promoter across individual cells (**Fig. 8c**). This result demonstrates that the region is accessible, and coaccessible with the *Pdyn* promoter, *in vivo*. Furthermore, this dataset suggests that the *Pdyn* enhancer is functional in the adult rat brain in selected cell populations that also express *Pdyn* mRNA.

DISCUSSION

Here we used transcriptomic and epigenomic profiling to characterize activity-dependent transcriptional and epigenomic waves in cultured embryonic rat striatal neurons, an *in vitro* model relevant for studying striatal function and neuropsychiatric disease. These experiments characterized a well-studied IEG expression program, which consisted primarily of activity-dependent transcription factors,

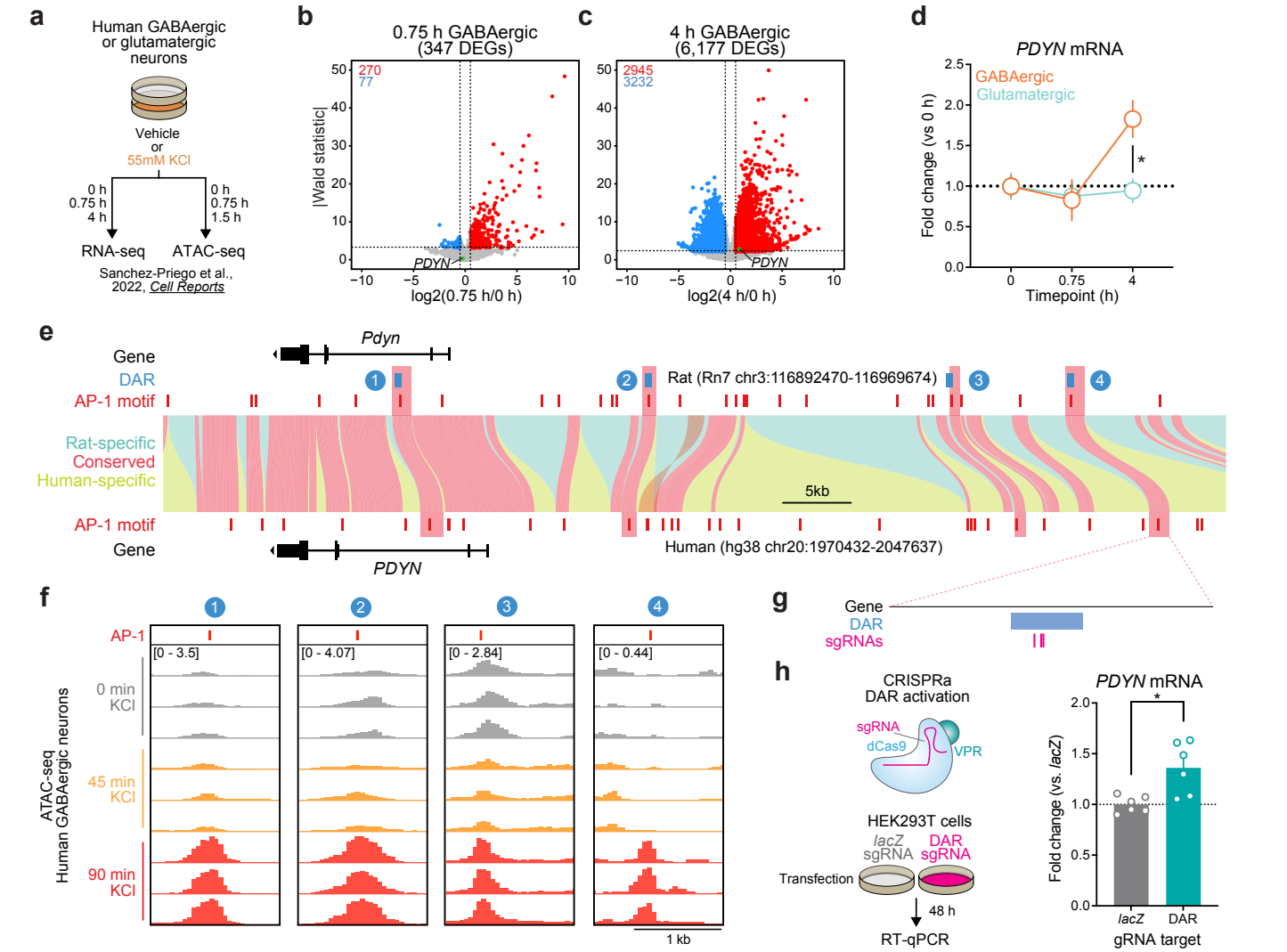

Figure 7. Identification and validation of a conserved *PDYN* enhancer in the human genome. **a**, Experimental design for published RNA-seq and ATAC-seq datasets from human GABAergic and glutamatergic neurons treated with 55mM KCl. **b-c**, Volcano plots for human GABAergic neurons treated with 55mM KCl for 0.75 or 4 h. *PDYN* is a significant DEG at 4 h, but not 0.75 h. **d**, *PDYN* is significanly upregulated 4 h after a KCl stimulus, but only in GABAergic neurons. Two-way ANOVA with Tukey's multiple comparison's test. *p<0.05. **e**, Linear synteny view of the rat and human *Pdyn*/*PDYN* locus reveals shared conservation of 4 distinct activity-dependent DARs identified in rat striatal neurons. **f**, ATAC-seq tracks of GABAergic neurons treated with 55mM KCl for 0, 0.75, or 1.5 h at the human *PDYN* locus. Regions conserved between rats and humans undergo dynamic remodeling in human GABAergic cells at 1.5 h after stimulation. A region homologous to the rat *Pdyn* enhancer characterized in Figure 6 is 63.7 kb upstream of the human *PDYN* gene. **g**, Location of CRISPR sgRNAs in the human genome for CRISPR-based activation of the *PDYN* DAR in human cells. **h**, CRISPRa at the human *PDYN* DAR is sufficient to upregulate *PDYN* mRNA in HEK293T cells. Mann-Whitney test. *p<0.05.

as well as a delayed LRG expression program (**Fig. 1a-c**). While IEGs are required for cellular and behavioral adaptations, they control this process through the transcriptional regulation of LRGs. LRGs are both functionally and temporally distinct from IEGs. IEGs primarily encode transcription factors and co-activators, while LRGs encode opioid peptides, transporters, and other proteins involved in synaptic plasticity[5,6]. For example, FOS regulates transcriptional activation of the LRG *Scg2*[23], a gene that encodes several neuropeptides that regulate inhibitory plasticity[28]. IEGs, such as *Fos*, may regulate LRGs by their involvement in activity-dependent chromatin remodeling, as *Fos* mRNA induction is required for activity-dependent chromatin remodeling in dentate gyrus following neuronal stimulation[8]. Surprisingly, analysis of both transcriptomic and epigenomic data revealed a temporal decoupling between transcriptional activation of IEGs and chromatin remodeling. While 1 h of depolarization was sufficient to induce hundreds of transcriptional changes, genome-wide chromatin remodeling was only observed following 4 h of depolarization. This result contrasts with a previously published study that observed genome-wide chromatin remodeling in the mouse dentate gyrus following 1 h of electroconvulsive stimulation[29]. Differences in the temporal dynamics of activity dependent chromatin remodeling could be due to differences in both the cell type of interest (hippocampal vs. striatal), as well as the type of stimulation (electroconvulsive stimulation vs. depolarization). Nonetheless, our studies agree in that a significant proportion of regions undergoing remodeling become more accessible following stimulation (**Fig. 2c**).

The accepted model of activity-dependent transcription posits that LRG activation is dependent on IEGs. To this point, blocking *Fos* mRNA induction via shRNA in the dentate gyrus is sufficient to significantly attenuate activity-dependent chromatin remodeling[8].

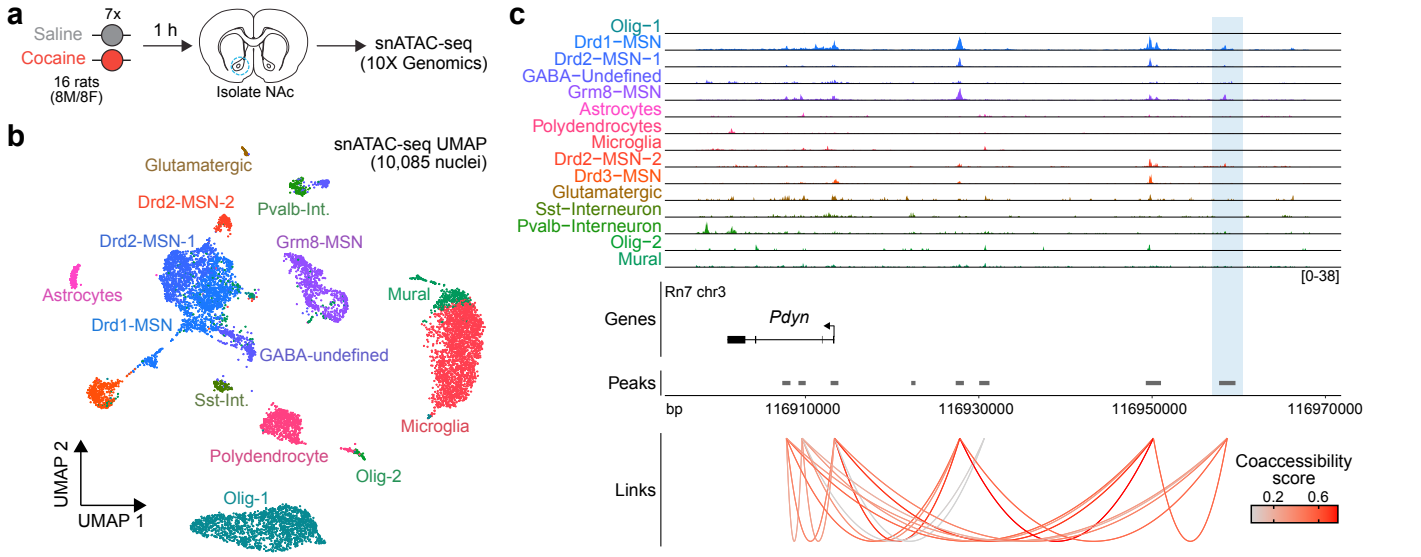

Figure 8. Characterization of the rat *Pdyn* DAR in the adult nucleus accumbens at single cell resolution. **a**, Experimental design. **b**, UMAP of 10,085 nuclei from adult rat nucleus accumens (NAc). **c**, Genome tracks displaying snATAC-seq data at the *Pdyn* locus. The experimentally validated *Pdyn* DAR (highlighted in blue) exhibits high co-accessibility with the proximal promoter for *Pdyn* as well as other nearby accessible regions.

This data demonstrates that *Fos* is required for some level of chromatin remodeling in the brain but does not provide evidence regarding the mechanisms through which it is involved. In non-neuronal cells, AP-1 acts as a pioneer factor at genomic enhancers by guiding the SWI/SNF chromatin remodeling complex to target regions[7,30]. Our data suggests a similar mechanism regulates activity-dependent chromatin remodeling at genomic enhancers in neurons. First, AP-1 motifs and FosB binding sites are significantly enriched within 4 h DARs (**Fig. 3b-d, S2e**). Second, blocking translation of IEGs, which include a significant number of AP-1 family members, completely blocks activity-dependent chromatin remodeling (**Fig. 4c,d**). Thus, we may propose a neuron-specific model in which neuronal stimulation results in the transcription and translation of AP-1 family members. These AP-1 family members then interact with the SWI/SNF complex to induce chromatin remodeling at genomic enhancers. However, while AP-1 is thought to aid in enhancer selection, it is expressed in a non-cell type specific manner and must choose from over 1 million potential AP-1 motifs in the genome. Thus, additional factors must be present to ensure precise cell type-specific responses to activity. The use of the HOMER database allowed us to explore the enrichment of over 400 additional transcription factor motifs, including ISL1, an MSN-selective transcription factor. ISL1 is significantly enriched in DARs (**Fig. 3c-d**). The combined enrichment of AP-1 and ISL1 at 4 h DARs suggests that cell type-specific transcription factors may be working in conjunction with activity-dependent transcription factors to induce chromatin remodeling. We envision three possible mechanisms through which cell type-specific transcription factors may be involved in this process. First, population-specific transcription factors may be directly interacting with AP-1 or chromatin remodeling complexes to induce remodeling at these sites. Second, ISL1 may stochastically bind these regions, resulting in specific temporal windows in which AP-1 might bind in a cooperative fashion. Finally, because cell type specific transcription factors are often activated during development, they may epigenetically alter potential binding sites proximal to AP-1 motifs, resulting in a preferential targeting of these AP-1 motifs at later timepoints. Any of these mechanisms would allow distinct cell types to induce specific LRG programs, even with homogenous IEG activation, and ultimately enable the same stimulus to produce different cellular adaptations in different cell types.

Multiple studies have demonstrated that most regions undergoing activity-dependent chromatin remodeling are genomic enhancers[7,29]. Analysis of 4 h DARs from this study identified a significant enrichment for DARs in non-coding regions and a depletion in coding regions (**Fig. 2d-e**), suggesting that activity dependent chromatin remodeling in striatal neurons is also occurring at genomic enhancers. This data also demonstrates a distinction between the chromatin profiles of IEG and LRG enhancers. IEG enhancers are "poised" at baseline, while LRG enhancers are largely inaccessible in without stimulation. For example, enhancers within the *Fos* locus are accessible in both vehicle and KCl treated samples (**Fig. S3**), while the *Pdyn* enhancer is only accessible with neuronal depolarization (**Fig. 5a**). In addition, LRG enhancers contain motifs for activity-dependent transcription factors (**Fig. 3a-e)** and are dependent on *de novo* protein translation (**Fig. 4c,d**). While LRG enhancers become accessible only with activity, both IEG and LRG enhancers are in noncoding regions of the genome and are marked by specific histone modifications like H3K27ac and H3K4me1[13,29,31,32] (**Fig. S2**).

While the enrichment of DARs in putative enhancer elements is intriguing, we also wanted to understand whether enhancers regulate nearby LRGs. To do this, we identified a DAR upstream of the *Pdyn* TSS that may serve as a functional enhancer. This

region is also accessible in the adult rat NAc (**Fig. 8c**). Furthermore, this region is coaccessible with the *Pdyn* promoter and has the highest level of accessibility in Drd1- and Grm8-MSNs, suggesting that the enhancer is functional *in vivo* and may exhibit some level of cell type specificity (**Fig. 8c**). However, a larger dataset containing more nuclei will be needed to test for any drug-specific chromatin remodeling at this region. CRISPR-based functional assays demonstrated that the DAR upstream of the *Pdyn* TSS serves as a genomic enhancer that is necessary, sufficient, and specific for transcription of *Pdyn*. We were particularly interested in *Pdyn* because it encodes the dynorphin neuropeptides that are agonists for the kappa opioid receptor[33]. The kappa opioid receptor system has been the target of several antagonists that reduce drug-taking behaviors in pre-clinical models[34–37]. Identification of a novel genomic enhancer for *Pdyn* would represent a novel therapeutic target. Furthermore, *Pdyn* is regulated by dopamine[38] and drugs of abuse[39–44], and polymorphisms and structural variants within the human *PDYN* gene locus are associated with drug abuse[45,46]. In particular, one polymorphism affects an AP-1 binding site within the *PDYN* gene promoter, which may result in less *PDYN* transcription and an increased risk for cocaine dependence[45]. Thus, the identification of a functional, conserved enhancer for *PDYN* in the human genome provides a novel potential therapeutic target capable of regulating stimulus-dependent changes in *PDYN* expression while leaving constitutive expression patterns unaltered. Future experiments should investigate whether this conserved enhancer element mediates reward-related behaviors and cellular adaptations.

In conclusion, we have identified and characterized temporally distinct waves of transcription and chromatin remodeling in striatal neurons. Furthermore, we found that the translation of IEGs is required for activity-dependent chromatin remodeling, particularly at genomic enhancers. Targeted analysis of LRG loci identified a genomic enhancer that is necessary, sufficient, and specific for *Pdyn* transcription. This enhancer is conserved in the human genome and represents a novel therapeutic target for modulation of the kappa opioid receptor system. Continued functional validation of putative enhancer regions within this dataset may provide additional therapeutic targets.

METHODS

Animals. Male or female adult rats were co-housed in pairs in plastic filtered cages with nesting enrichment in an Association for Assessment and Accreditation of Laboratory Animal Care–approved animal care facility maintained between 23° and 24°C on a 12-hour light/12-hour dark cycle with ad libitum food (Lab Diet Irradiated rat chow) and water. Bedding and enrichment were changed weekly by animal resources program staff. Animals were randomly assigned to experimental groups. All experiments were approved by the University of Alabama at Birmingham Institutional Animal Care and Use Committee (IACUC). Timed pregnant dams were individually housed until embryonic day 18 when striatal cultures were generated as previously described[9,25,32].

Neuronal cell culture. Cells were maintained in neurobasal media supplemented with B27 and LG for 11-12 days in vitro (DIV) with half media changes on DIV 1, 5-6, and 9-10. For depolarization experiments neurons were treated with KCl dissolved in neurobasal media to a final concentration of 10mM for 1 or 4 h. To test the necessity of protein translation in mediating activity dependent transcription and chromatin remodeling, anisomycin was dissolved in DMSO and treated to a final concentration of 40μM for 30 minutes prior to depolarization.

HEK-293T experiments. HEK-293T cells were maintained in DMEM + 10% FBS and plated at 80,000 cells/well in 24 well plates. 24 h later cells were transfected with Fugene HD (Promega) and constructs containing dCas9-VPR and gRNA vectors targeting the conserved DAR region (500ng plasmid DNA in molar ratios sgRNA:dCas9-VPR). 48 h later, cells were lysed and RNA was extracted.

CRISPR/dCas9 gRNA design and delivery. Guide RNAs targeting *lacZ*, the rat *Pdyn* enhancer, and conserved human *PDYN* enhancer were designed using CHOPCHOP as previously described[9,24,25,32,47]. CRISPR/dCas9 and gRNA constructs were packaged into lentiviral vectors and transduced as previously described[9,24,47–49]. gRNA sequences can be found in **Table S4**.

RNA extraction and RT-qPCR. RNA extractions, cDNA synthesis, and RT-qPCR were performed as previously described[9,25,32,49]. All RT-qPCR primers can be found in **Table S4**.

Western blotting. DIV11-12 cultured rat embryonic striatal neurons were treated with 40μM Anisomycin followed by 4 h of depolarization with 10mM KCl in 12 well plates. Following depolarization, media was removed, and wells were washed with 1x TBS. Cells were lysed using RIPA lysis buffer (50mM Tris-HCl pH 8, 150 mM NaCl, 1% NP-40 Substitute, 0.5% Sodium Deoxycholate, 0.1% SDS, 1X HALT protease inhibitor cocktail). Following protein separation and transfer, PVDF membrane was incubated with FOS primary antibody (Cell Signaling Cat. No. 9F6, 1:1000 in TBST) and β-tubulin primary antibody (Millipore Cat. No. 05-661 1:2000 in TBST) overnight at 4°C. Following primary antibody incubation, secondary antibodies (IRDye 680RD Goat Anti-Rabbit Cat. No. 926-68071 1:10000 in TBST and IRDye 800CW Donkey Anti-Mouse Cat. No. 926-32212 1:10000 in 1:1 TBST:Intercept blocking

buffer with 0.02% SDS) for 1 h at room temperature. Imaging was performed using a Licor Odyssey imager.

RNA-Seq library preparation and analysis. RNA was extracted from cultured rat embryonic striatal neurons following stimulation (RNeasy, Qiagen) and submitted to the Genomics core lab at the Heflin Center for Genomic Sciences at the University of Alabama at Birmingham for library preparation as previously described[9,32]. 75bp paired-end libraries were sequenced using the NextSeq500. Paired-end FASTQ files were analyzed using a custom bioinformatics pipeline built with Snakemake[50] (v6.1.0). Briefly, read quality was assessed using FastQC before and after trimming with Trim_Galore![51] (v0.6.7). Splice-aware alignment to the mRatBn7.2/Rn7 reference assembly for cultured embryonic rat striatal neurons using the associated Ensembl gene transfer format (gtf) file (version 105) and the Hg38 reference assembly using the associated Ensembl gtf (version 99) for previously published human datasets was performed with STAR[52] (v2.7.9a). Binary alignment map (BAM) files were indexed with SAMtools[53] (v1.13). Gene-level counts were generated using the featureCounts function within the Rsubread package[54] (v2.6.1) in R (v4.1.1). QC metrics were collected and reviewed with MultiQC[55] (v1.11). Differential expression testing was conducted using DeSeq2[56] (v1.38.3). DEG testing *p*-values were adjusted with the Benjamini-Hochberg method[57]. DEGs were designated as those genes with an adjusted p-value < 0.05 and a |log2FoldChange| > 0.5. Molecular function and cellular component GO terms were identified by first characterizing upregulated DEGs specific for the 1 h or 4 h timepoint. Ensembl gene IDs for all genes were input into gProfiler[10] with a custom background of all expressed genes (counts > 0). Resulting *p*-values were adjusted with the Benjamini-Hochberg[57] method.

ATAC-Seq library preparation and analysis. ATAC-Seq libraries were prepared as previously described[32]. 75bp paired-end libraries were then sequenced using the NextSeq500 at the Genomics core lab at the Heflin Center for Genomic Sciences at the University of Alabama at Birmingham as previously described[32]. Paired-end FASTQ files were analyzed using a custom bioinformatics pipeline built with Snakemake[50] (v6.1.0). Read quality was assessed with FastQC before and after trimming (trimming was performed with Trim_Galore![51] v0.6.7). Particularly, Nextera adapters (5'-CTGTCTCTTATA-3') were identified and removed. FASTQ files were then aligned using Bowtie2[58] (v2.4.4) with the Ensembl gene transfer format (gtf) file (version 105) and the Hg38 reference assembly using the associated Ensembl gtf (version 99) for previously published human datasets. PCR duplicates were marked with using Picard[59] (v2.26.2). For human ATAC-seq data, encode version 4 of the Hg38 blacklist was used. PCR duplicates, in addition to reads mapping to the mitochondrial genome, were removed using SAMtools[53] (v1.13). BigWig files were generated with deeptools[60] v3.5.1. QC metrics were collected and reviewed with MultiQC[55] (v1.11). For ATAC-Seq libraries from cultured rat embryonic striatal neurons, peaks were called using MACS2[61] (v 2.1.1.20160309) callpeak with options - -qvalue 0.01 - -gsize 2626580772 - -format BAMPE. Differential accessibility analysis was performed with Diffbind[62] (v3.8.4). DARs were defined as regions with an adjusted *p*-value ≤ 0.05. Reads within peaks were counted using the dba.count() function with options bParallel=TRUE, summits=250, bUseSummarizeOverlaps=TRUE, and score = DBA_SCORE_TMM_READS_FULL_CPM. Motif enrichment was investigated using HOMER[16] (v4.11.1) findMotifsGenome.pl. Dimensionality reduction of motif enrichment across all DARs was conducted using the umap package in R (v2.10.0) to calculate 10 UMAP[20] components with custom options min_dist=1e-250, n_neighbors =30, and n_components = 10. UMAP values were used to cluster points with the hdbscan() function of the dbscan[21] package (v1.1-11) with minPts=150.

Pseudotime. Pseudotime calculations were performed using Monocle v3_1.3.1[63] and Seurat v4.3.0[64]. A Seurat object containing Drd1-MSNs from male and female adult Sprague-Dawley rats treated with a single cocaine injection[22] was subject to the standard dimensionality reduction and clustering workflow using 17 principal components and a resolution value of 0.2. Annotation, counts metadata, and cell barcode information were extracted from the Seurat object and reconstructed into a Monocle v3 cds object using new_cell_data_set(). Rather than reclustering, the UMAP coordinates were extracted from the Seurat object and added to the Monocle object. The trajectory graph was created using learn_graph() and the root cell was chosen in the "inactivated" population that expressed *Drd1* and *Htr4*[27]. Pseudotime values for each cell were exported from the cds object and added back to the Seurat object metadata.

Gene regulatory network reconstruction. Reconstruction of gene regulatory networks within *Drd1*-MSNs was performed using Epoch[65]. Dynamically expressed genes were found using findDynGenes(), and a *p*-value threshold of 0.05 was used to filter for significance. Transcription factors for *R. norvegicus* were downloaded from AnimalTFDB4.0[66] used to construct an initial static network using reconstructGRN(). Epoch uses a Context Likelihood of Relatedness (CLR) model to infer relationships between transcription factors (TFs) and transcription targets (TGs) using transcriptomic information and calculated pseudotime values. A process which Epoch terms as "crossweighting" was then performed to filter out indirect relationships or non-logical connections. Next, a dynamic network was extracted by fractionating the *Drd1* cells by "epochs", which is based on pseudotime. TF to TG relationships were ranked using PageRank[67].

Single nucleus dissociation. Flash-frozen NAc tissue was added to a tube containing 500µl lysis buffer (1mM Tris-HCl pH 7.4, 1mM NAc, 0.3 mM MgCl2, 0.01% Tween-20, 0.01% Igepal in nuclease free water, 0.001% Digitonin, 0.1% BSA), homogenized using a motorized homogenizer and RNase free pestle, and incubated on ice for 5 minutes. Samples were then pipette mixed 15x and incubated on ice for an additional 10 minutes. Following lysis, 4 samples from same sex and treatment were grouped into a single sample, and 2mL chilled wash buffer (10mM Tris-HCl pH 7.4, 10mM NACl, 3mM MgCl2, 1% BSA, 0.1% Tween-20) was added. Samples were then passed through 70µM and 40µM Scienceware Flowmi Cell Strainers. Samples were then centrifuged at 250 rcf for 5 min at 4°C. Supernatant was removed and the pellet was resuspended in 1mL of chilled wash buffer (10mM Tris-HCl pH 7.4, 10mM NACl, 3mM MgCl2, 1% BSA, 0.1% Tween-20). 100µL of sample was then stained with 7-aminoactinomycin D and used to set a representative gate for fluorescence activated cell sorting (FACs). This gate was then used to purify nuclei further. Following FACs, samples were spun at 250 rcf for 10 min at 4°C to remove any remaining debris. Samples were then loaded into individual wells of the Chromium NextGem Single Cell Chip using 4 of the 8 available wells.

snATAC-seq alignment and object construction. 10X Genomics snATAC-seq libraries were generated from male and female Sprague-Dawley rats exposed injected with 20 mg/kg cocaine (or saline control) once daily for seven days. snATAC-seq data was aligned to the mRatBN7.2/Rn7 reference assembly using cellranger-atac v2.1.0 and the procedure outlined by 10X Genomics[68]. Analysis of the cellranger-atac output was analyzed using Signac v1.9.0[69] and Seurat v4.3.0[64]. Counts, fragments, and barcode information for each treatment group were loaded and combined into Seurat objects as outlined by the Stuart lab website (https://stuartlab.org/signac/). The groups were then merged into one object based on a common set of features and the standard Signac dimensionality reduction and clustering workflow was performed using 2:30 dimensions and a resolution value of 0.2. Data was then integrated with the snRNA-seq data from the same samples. Common anchors between the two were used to predict and label the cell types present in the snATAC-seq data.

Coaccessibility analysis. Detection of cis-co-accessible sites in the snATAC-seq data was performed using Cicero v1.3.9[70] and Monocle v3_1.3.1[63]. The finalized snATAC-seq Seurat object was first converted into a Monocle3 cds object and then converted into a Cicero object. The Cicero connections were found using run_cicero with the Cicero object and a dataframe containing chromosome lengths extracted from the Seurat object. Cis-coaccessible networks were then calculated using generate_ccans(), and the produced links were added back to the starting Seurat object.

DATA AVAILABILITY

All relevant data that support the findings of this study are available by request from the corresponding author (J.J.D.). Sequencing data that support the findings of this study are available in Gene Expression Omnibus. Accession numbers of specific datasets are outlined below.

Bulk RNA-seq primary rat striatal neurons 1 h vehicle or KCl: GSE150499
Bulk RNA-seq primary rat striatal neurons 4 h vehicle or KCl: GSE233752
Bulk ATAC-seq primary rat striatal neurons 1 h vehicle or KCl: GSE150589
Bulk ATAC-seq primary rat striatal neurons 4 h vehicle or KCl: GSE233368
Bulk ATAC-seq primary rat striatal neurons 4 h vehicle or KCl with anisomycin: GSE233368
snATAC-seq adult rat nucleus accumbens: GSE233754

ACKNOWLEDGEMENTS

We thank all current and former Day Lab members for assistance and support. This work was supported by NIH grants DP1DA039650, R01MH114990, R01DA053743, R01DA054714, and the McKnight Foundation Neurobiology of Brain Disorders Award (JJD). L.I. is supported by the Civitan International Research Center at UAB. R.A.P.III is supported by the AMC21 scholar program and the UAB T32 in the Neurobiology of Cognition and Cognitive Disorders (T32NS061788). We acknowledge support from the University of Alabama at Birmingham Biological Data Science Core (RRID:SCR_021766), and the UAB Heflin Center for Genomic Sciences.

AUTHOR CONTRIBUTIONS

R.A.P.III and J.J.D. conceived of experiments. R.A.P.III performed all experiments. D.R. assisted with HEK293T experiments. R.A.P.III and J.J.T conducted the single nucleus dissociation for snATAC experiments. R.A.P.III analyzed next generation sequencing data with assistance from E.W. and L.I. R.A.P.III and J.J.D wrote the manuscript. All authors have approved the final version of the manuscript.

CONFLICTS OF INTEREST

The authors declare no competing interests.

REFERENCES

1. Mews, P., Walker, D. M. & Nestler, E. J. Epigenetic priming in drug addiction. *Cold Spring Harb. Symp. Quant. Biol.* **83,** 131–139 (2018).
2. Adinoff, B. Neurobiologic processes in drug reward and addiction. *Harv. Rev. Psychiatry* **12,** 305–320 (2004).
3. Ebert, D. H. & Greenberg, M. E. Activity-dependent neuronal signalling and autism spectrum disorder. *Nature* **493,** 327–337 (2013).
4. Zhang, Z. *et al.* Autism-Associated Chromatin Regulator Brg1/SmarcA4 Is Required for Synapse Development

and Myocyte Enhancer Factor 2-Mediated Synapse Remodeling. *Mol. Cell. Biol.* **36,** 70–83 (2016).
5. Yap, E.-L. & Greenberg, M. E. Activity-Regulated Transcription: Bridging the Gap between Neural Activity and Behavior. *Neuron* **100,** 330–348 (2018).
6. Tyssowski, K. M. *et al.* Different neuronal activity patterns induce different gene expression programs. *Neuron* **98,** 530–546.e11 (2018).
7. Vierbuchen, T. *et al.* AP-1 Transcription Factors and the BAF Complex Mediate Signal-Dependent Enhancer Selection. *Mol. Cell* **68,** 1067–1082.e12 (2017).
8. Su, Y. *et al.* Neuronal activity modifies the chromatin accessibility landscape in the adult brain. *Nat. Neurosci.* **20,** 476–483 (2017).
9. Savell, K. E. *et al.* A dopamine-induced gene expression signature regulates neuronal function and cocaine response. *Sci. Adv.* **6,** eaba4221 (2020).
10. Raudvere, U. *et al.* g:Profiler: a web server for functional enrichment analysis and conversions of gene lists (2019 update). *Nucleic Acids Res.* **47,** W191–W198 (2019).
11. Feng, J. *et al.* Chronic cocaine-regulated epigenomic changes in mouse nucleus accumbens. *Genome Biol.* **15,** R65 (2014).
12. Sciumè, G. *et al.* Rapid Enhancer Remodeling and Transcription Factor Repurposing Enable High Magnitude Gene Induction upon Acute Activation of NK Cells. *Immunity* **53,** 745–758.e4 (2020).
13. Carullo, N. V. N. & Day, J. J. Genomic enhancers in brain health and disease. *Genes (Basel)* **10,** 43 (2019).
14. Chen, L.-F. *et al.* Enhancer Histone Acetylation Modulates Transcriptional Bursting Dynamics of Neuronal Activity-Inducible Genes. *Cell Rep.* **26,** 1174–1188.e5 (2019).
15. Yeh, S.-Y. *et al.* Cell Type-Specific Whole-Genome Landscape of ΔFOSB Binding in the Nucleus Accumbens After Chronic Cocaine Exposure. *Biol. Psychiatry* (2023). doi:10.1016/j.biopsych.2022.12.021
16. Heinz, S. *et al.* Simple combinations of lineage-determining transcription factors prime cis-regulatory elements required for macrophage and B cell identities. *Mol. Cell* **38,** 576–589 (2010).
17. Shalizi, A. K. & Bonni, A. brawn for brains: the role of MEF2 proteins in the developing nervous system. *Curr Top Dev Biol* **69,** 239–266 (2005).
18. Dietrich, J.-B., Takemori, H., Grosch-Dirrig, S., Bertorello, A. & Zwiller, J. Cocaine induces the expression of MEF2C transcription factor in rat striatum through activation of SIK1 and phosphorylation of the histone deacetylase HDAC5. *Synapse* **66,** 61–70 (2012).
19. Ehrman, L. A. *et al.* The LIM homeobox gene Isl1 is required for the correct development of the striatonigral pathway in the mouse. *Proc. Natl. Acad. Sci. USA* **110,** E4026-35 (2013).
20. McInnes, L., Healy, J. & Melville, J. UMAP: Uniform Manifold Approximation and Projection for Dimension Reduction. *arXiv* (2018). doi:10.48550/arxiv.1802.03426
21. Hahsler, M., Piekenbrock, M. & Doran, D. dbscan : Fast Density-Based Clustering with *R. J. Stat. Softw.* **91,** (2019).
22. Phillips, R. A. *et al.* Distinct subpopulations of D1 medium spiny neurons exhibit unique transcriptional responsiveness to cocaine. *Mol. Cell. Neurosci.* **125,** 103849 (2023).
23. Yap, E. L. *et al.* Bidirectional perisomatic inhibitory plasticity of a Fos neuronal network. *Nature* **590,** 115–121 (2020).
24. Duke, C. G. *et al.* An improved crispr/dcas9 interference tool for neuronal gene suppression. *Front. Genome Ed.* **2,** 9 (2020).
25. Savell, K. E. *et al.* A Neuron-Optimized CRISPR/dCas9 Activation System for Robust and Specific Gene Regulation. *eNeuro* **6,** (2019).
26. Sanchez-Priego, C. *et al.* Mapping cis-regulatory elements in human neurons links psychiatric disease heritability and activity-regulated transcriptional programs. *Cell Rep.* **39,** 110877 (2022).
27. Phillips, R. A. *et al.* Distinct subpopulations of D1 medium spiny neurons exhibit unique transcriptional responsiveness to cocaine. *BioRxiv* (2023). doi:10.1101/2023.01.12.523845
28. Iwase, K. *et al.* The secretogranin II gene is a signal integrator of glutamate and dopamine inputs. *J. Neurochem.* **128,** 233–245 (2014).
29. Malik, A. N. *et al.* Genome-wide identification and characterization of functional neuronal activity-dependent enhancers. *Nat. Neurosci.* **17,** 1330–1339 (2014).
30. Wolf, B. K. *et al.* Cooperation of chromatin remodeling SWI/SNF complex and pioneer factor AP-1 shapes 3D enhancer landscapes. *Nat. Struct. Mol. Biol.* **30,** 10–21 (2023).
31. Zentner, G. E., Tesar, P. J. & Scacheri, P. C. Epigenetic signatures distinguish multiple classes of enhancers with distinct cellular functions. *Genome Res.* **21,** 1273–1283 (2011).
32. Carullo, N. V. N. *et al.* Enhancer RNAs predict enhancer-gene regulatory links and are critical for enhancer function in neuronal systems. *Nucleic Acids Res.* **48,** 9550–9570 (2020).
33. Chavkin, C., James, I. F. & Goldstein, A. Dynorphin is a specific endogenous ligand of the kappa opioid receptor. *Science* **215,** 413–415 (1982).
34. Prisinzano, T. E., Tidgewell, K. & Harding, W. W. Kappa opioids as potential treatments for stimulant dependence. *AAPS J.* **7,** E592-9 (2005).
35. Zamarripa, C. A. *et al.* Kappa opioid agonists reduce oxycodone self-administration in male rhesus monkeys. *Psychopharmacology* **237,** 1471–1480 (2020).
36. Chavkin, C. The therapeutic potential of κ-opioids for treatment of pain and addiction. *Neuropsychopharmacology* **36,** 369–370 (2011).
37. Valenza, M., Windisch, K. A., Butelman, E. R., Reed, B. & Kreek, M. J. Effects of Kappa opioid receptor blockade by LY2444296 HCl, a selective short-acting antagonist, during chronic extended access cocaine self-administration and re-exposure in rat. *Psychopharmacology* **237,** 1147–1160 (2020).
38. Berke, J. D., Paletzki, R. F., Aronson, G. J., Hyman, S. E. & Gerfen, C. R. A complex program of striatal gene expression induced by dopaminergic stimulation. *J. Neurosci.* **18,** 5301–5310 (1998).
39. Cole, R. L., Konradi, C., Douglass, J. & Hyman, S. E. Neuronal adaptation to amphetamine and dopamine: molecular mechanisms of prodynorphin gene regulation in rat striatum. *Neuron* **14,** 813–823 (1995).
40. Jenab, S. *et al.* Effects of cocaine on c-fos and preprodynorphin mRNA levels in intact and ovariectomized Fischer rats. *Brain Res. Bull.* **58,** 295–299 (2002).

41. Sun, H., Luessen, D. J., Kind, K. O., Zhang, K. & Chen, R. Cocaine Self-administration Regulates Transcription of Opioid Peptide Precursors and Opioid Receptors in Rat Caudate Putamen and Prefrontal Cortex. *Neuroscience* **443,** 131–139 (2020).
42. Corchero, J., Avila, M. A., Fuentes, J. A. & Manzanares, J. Δ-9-Tetrahydrocannabinol increases prodynorphin and proenkephalin gene expression in the spinal cord of the rat. *Life Sci.* **61,** PL39-PL43 (1997).
43. Piechota, M. *et al.* Common transcriptional effects in the mouse striatum following chronic treatment with heroin and methamphetamine. *Genes Brain Behav.* **11,** 404–414 (2012).
44. Carlezon, W. A. *et al.* Regulation of cocaine reward by CREB. *Science* **282,** 2272–2275 (1998).
45. Yuferov, V. *et al.* A functional haplotype implicated in vulnerability to develop cocaine dependence is associated with reduced PDYN expression in human brain. *Neuropsychopharmacology* **34,** 1185–1197 (2009).
46. Clarke, T. K. *et al.* Genetic association analyses of PDYN polymorphisms with heroin and cocaine addiction. *Genes Brain Behav.* **11,** 415–423 (2012).
47. Carullo, N. V. N. *et al.* A Cre-Dependent CRISPR/dCas9 System for Gene Expression Regulation in Neurons. *eNeuro* **8,** (2021).
48. Carullo, N. V. N., Revanna, J. S., Tuscher, J. J., Bauman, A. J. & Day, J. J. A Cre-dependent CRISPR/dCas9 activation system for gene expression regulation in neurons. *BioRxiv* (2020). doi:10.1101/2020.11.20.391987
49. Savell, K. E., Sultan, F. A. & Day, J. J. A Novel Dual Lentiviral CRISPR-based Transcriptional Activation System for Gene Expression Regulation in Neurons. *Bio Protoc* **9,** (2019).
50. Mölder, F. *et al.* Sustainable data analysis with Snakemake. *F1000Res.* **10,** 33 (2021).
51. Martin, M. Cutadapt removes adapter sequences from high-throughput sequencing reads. *EMBnet j.* **17,** 10 (2011).
52. Dobin, A. *et al.* STAR: ultrafast universal RNA-seq aligner. *Bioinformatics* **29,** 15–21 (2013).
53. Li, H. *et al.* The Sequence Alignment/Map format and SAMtools. *Bioinformatics* **25,** 2078–2079 (2009).
54. Liao, Y., Smyth, G. K. & Shi, W. The R package Rsubread is easier, faster, cheaper and better for alignment and quantification of RNA sequencing reads. *Nucleic Acids Res.* **47,** e47 (2019).
55. Ewels, P., Magnusson, M., Lundin, S. & Käller, M. MultiQC: summarize analysis results for multiple tools and samples in a single report. *Bioinformatics* **32,** 3047–3048 (2016).
56. Love, M. I., Huber, W. & Anders, S. Moderated estimation of fold change and dispersion for RNA-seq data with DESeq2. *Genome Biol.* **15,** 550 (2014).
57. Benjamini, Y. & Hochberg, Y. Controlling the false discovery rate: a practical and powerful approach to multiple testing. *Journal of the Royal Statistical Society: Series B (Methodological)* **57,** 289–300 (1995).
58. Langmead, B. & Salzberg, S. L. Fast gapped-read alignment with Bowtie 2. *Nat. Methods* **9,** 357–359 (2012).
59. Broad Institute. *Picard toolkit*. (Broad Institute, 2018).
60. Ramírez, F. *et al.* deepTools2: a next generation web server for deep-sequencing data analysis. *Nucleic Acids Res.* **44,** W160-5 (2016).
61. Zhang, Y. *et al.* Model-based analysis of ChIP-Seq (MACS). *Genome Biol.* **9,** R137 (2008).
62. Ross-Innes, C. S. *et al.* Differential oestrogen receptor binding is associated with clinical outcome in breast cancer. *Nature* **481,** 389–393 (2012).
63. Cao, J. *et al.* The single-cell transcriptional landscape of mammalian organogenesis. *Nature* **566,** 496–502 (2019).
64. Hao, Y. *et al.* Integrated analysis of multimodal single-cell data. *Cell* **184,** 3573–3587.e29 (2021).
65. Su, E. Y., Spangler, A., Bian, Q., Kasamoto, J. Y. & Cahan, P. Reconstruction of dynamic regulatory networks reveals signaling-induced topology changes associated with germ layer specification. *Stem Cell Rep.* **17,** 427–442 (2022).
66. Shen, W.-K. *et al.* AnimalTFDB 4.0: a comprehensive animal transcription factor database updated with variation and expression annotations. *Nucleic Acids Res.* **51,** D39–D45 (2023).
67. Brin, S. & Page, L. The anatomy of a large-scale hypertextual Web search engine. *Computer Networks and ISDN Systems* **30,** 107–117 (1998).
68. Satpathy, A. T. *et al.* Massively parallel single-cell chromatin landscapes of human immune cell development and intratumoral T cell exhaustion. *Nat. Biotechnol.* **37,** 925–936 (2019).
69. Stuart, T., Srivastava, A., Madad, S., Lareau, C. A. & Satija, R. Single-cell chromatin state analysis with Signac. *Nat. Methods* **18,** 1333–1341 (2021).
70. Pliner, H. A. *et al.* Cicero Predicts cis-Regulatory DNA Interactions from Single-Cell Chromatin Accessibility Data. *Mol. Cell* **71,** 858–871.e8 (2018).

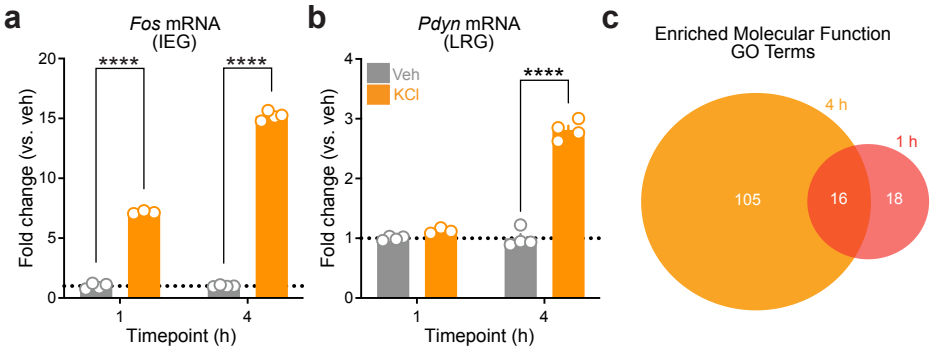

Figure S1. IEGs and LRGs are temoporally and functionally distinct. **a-b**, Plots demonstrating activation of IEGs at both 1 and 4 hours after depolarization, while LRGs are only activated after 4 hours of stimulation. Two-way ANOVA with Tukey's multiple comparisons test.****p<0.0001. **c**, Venn diagram comparing molecular function GO terms enriched in 1 and 4 hour DEG lists.

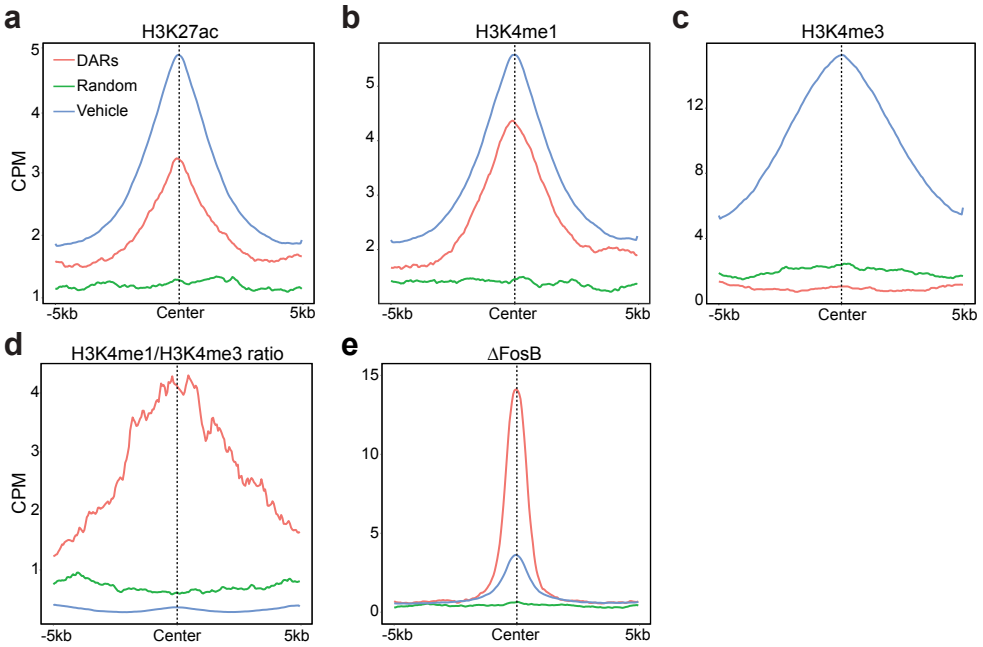

Figure S2. Transcription factor binding and histone modifications in 4 h DARs, random regions, and vehicle peaks. Enrichment plots for **a**, H3K27ac, **b**, H3K4me1, **c**, H3K4me3, **d**, H3K4me1/H3K4me3. **e**, ΔFosB. Data from Yeh, et al., 2023 *Biological Psychiatry*.

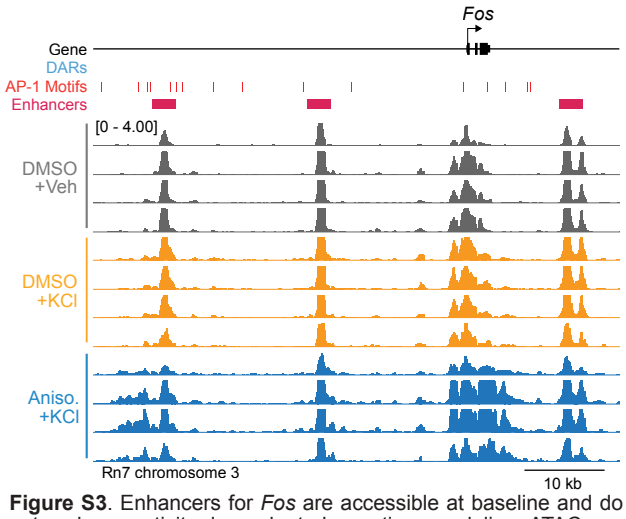

Figure S3. Enhancers for *Fos* are accessible at baseline and do not undergo activity-dependent chromatin remodeling. ATAC-seq tracks at the *Fos* locus for neurons treated with DMSO + Veh, DMSO + KCl, or Anisomycin + KCl for 4 h.

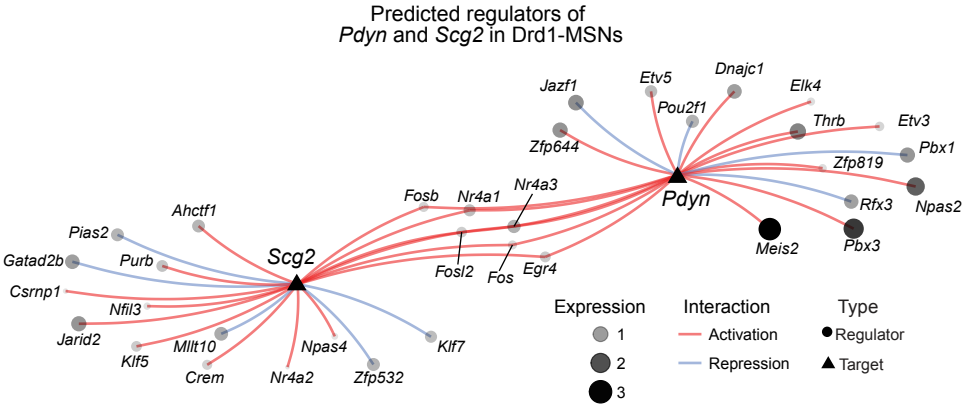

Figure S4. Predicted regulators of *Pdyn* and *Scg2* in Drd1-MSNs. Reconstruction of gene regulatory networks in Drd1-MSNs predicts AP-1 family members such as *Fos* and *Fosb* regulate both *Scg2* and *Pdyn*.

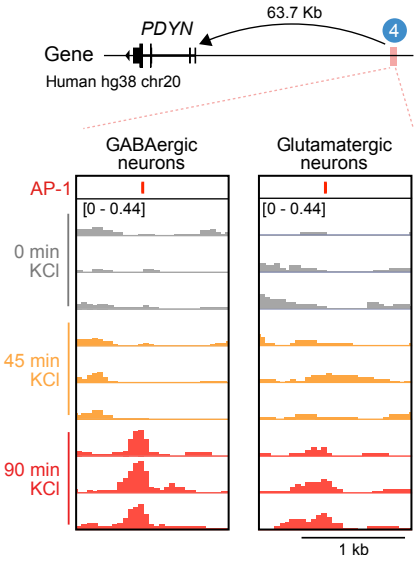

Figure S5. Conserved activity-regulated *PDYN* DAR is selective for GABAergic neurons. ATAC-seq tracks from human induced GABAergic and Glutamaterigc neurons treated with 55mM KCl for 0, 0.75, or 1.5 h. Data from Sanchez-Priego, et al., 2022 *Cell Reports*.